Nanoscale Advances

ROYAL SOCIETY OF CHEMISTRY

PAPER

View Article Online
View Journal | View Issue

Cite this: *Nanoscale Adv.*, 2024, **6**, 3923

Subcritical water digestion of woody biomass: extraction of cellulose nanomaterials under acid-lean condition†

Ruby Osei-Bonsu, [ab] Mahfuzul Hoque,[ab] Philip S. McMichael[ab] and E. Johan Foster *[ab]

Subcritical water extraction (SWE) is an emerging green and efficient hydrothermal technology, that offers superior performance in active material extraction, scalability, and reduction of harsh process chemicals, in biomass conversion. Regarding biomaterials, traditional isolation methods for cellulose nanocrystals (CNCs) are reliant on harsh chemicals (*i.e.*, strong acid), which are expensive with little to no recyclability. This paper explores SWE as a nanotechnology platform to produce CNCs under the principle of "less is more" — by using low content (1 wt%) of phosphoric acid under subcritical conditions. Acid-catalyzed digestion of woody biomass afforded CNCs desirable physico-chemical features that are dependent on the process parameters (temperature, pressure, and time). Process temperature had a major impact on the reduction of fiber sizes (macroscale to nanoscale), fiber degradation, and fiber coloration (white to black). Electron microscopy revealed rod-like structures, with varying particle size distribution (100–500 nm), dominated by process time. However, colloidal stability was low (*versus* acid-hydrolyzed CNCs) due to the low charges on the surface of CNCs. Interestingly, vibrational spectroscopy reveals the effect of process pressure on biomass conversion to CNCs (with cellulose I structure) evidenced by Raman spectroscopy and solid-state fluorometry. The produced (bio)nanomaterials possessed a degree of crystallinity (~70%) comparable to those produced *via* acid hydrolysis, with higher thermal stability, enhancing their applicability over a wide range of heat-intensive processes required for nanocomposite applications in biomedical and automotive industries, among others.

Received 2nd February 2024
Accepted 13th June 2024

DOI: 10.1039/d4na00108g

rsc.li/nanoscale-advances

Introduction

Unprecedented climate change (*i.e.*, global warming) in recent years has triggered an upsurge in interest in utilizing woody biomass to extract useful and functional nanomaterials, *i.e.*, cellulose nanocrystals (CNCs). Woody biomass, generally derived from trees includes various forest and industrial residues[1] which are primarily comprised of cellulose, the most abundant polymer on earth, known for its renewability, biodegradability, and biocompatibility. Cellulose as a biopolymer exists as a linear chain polymer, consisting of repeating glucose monomers linked together by β-1-4 glycosidic linkages arranged into amorphous and crystalline regions. Naturally existing as fibers, the structure of cellulose can be broken down into smaller fibers[2] known as cellulose nanofibers at the nanoscale with lengths often extending to several micrometres and widths between 5–60 nm.[3] Selective hydrolysis of cellulose nanofibers through an effective combination of mechanical, chemical, and or biological treatments results in the removal of the amorphous regions and subsequent isolation of the crystalline regions known as cellulose nanocrystals (CNCs or NCC). Nanocrystalline cellulose (NCC) can exist in the form of nanocrystals with lengths from 50–1000 nm, widths between 5–70 nm, and aspect ratios of 5–30, depending on conditions of isolation.[4,5] Owing to their attractive physical, mechanical, and rheological properties, CNCs have been exploited as natural stiff fillers for polymer composite reinforcement materials,[6] nanocarriers for bio-macromolecules and drugs,[7] and rheology modifiers.[8]

However, CNCs are traditionally isolated *via* the use of strong acid treatment (*e.g.*, sulfuric acid)[9–12] and biological routes, using cellulose digesting enzymes.[13,14] To achieve higher hydrolysis yields, several optimization studies have been reported with different acids. For instance, Beltramino *et al.* reported 62–65 wt% sulfuric acid for the highest conversion of cellulose.[15] Other works have reported 35–40 wt% and 70–80 wt% hydrochloric and phosphoric acids, respectively for efficient hydrolysis of cellulose.[16–19] However, the deployment of large volumes of these harsh chemicals renders the process less

[a]*Department of Chemical and Biological Engineering, University of British Columbia, Pulp and Paper Centre, 2385 East Mall, V6T 1Z4, Canada*
[b]*BioProducts Institute, University of British Columbia, 2385 East Mall, V6T 1Z4, BC, Canada. E-mail: johan.foster@ubc.ca*

† Electronic supplementary information (ESI) available. See DOI: https://doi.org/10.1039/d4na00108g

environmentally friendly. As such, hydrolyzing cellulose with diluted ionic liquids and inorganic acids has been investigated as an alternative to acid hydrolysis,[20] – not a cost-effective approach and difficult to recycle the solvent.

On the other hand, among the various sustainable extraction processes engineered recently is the unique use of water (as a green solvent) that is, subcritical water extraction (SWE)[21] – a hydrothermal process in which water is held above its vapor pressure to maintain its liquid form when heated above the standard boiling point (100 °C) and below the critical point (374 °C). Under these thermodynamic conditions, water exhibits two unique properties; a higher ion product *i.e.*, higher concentrations of H_3O^+ species[22] making water slightly acidic capable of catalyzing chemical reactions, and relatively low dielectric constant, increasing water's solubility to dissolve organic materials.[23] Thus, SWE offers an "eco-friendly", "non-toxic", and "effluent-free" nanotechnological platform, which has the potential to accelerate our efforts towards a circular bioeconomy.

We note that previously, SWE has been successfully deployed for "organic-solvent free" production of nano pharmaceuticals (*e.g.*, prednisolone),[24] development of thyme essential oil in water (O/W) nanoemulsions (food nanotechnology),[25] and liquefaction of biomass.[26] As an earlier adoption of this technology, CNCs were produced from microcrystalline cellulose (Avicel®PH-101, hereinafter abbreviated as MCC) by Novo *et al.*[21] It is important to note that MCC is already hydrolyzed (with hydrochloric acid) cellulose thus, in solid-state, it exists as a bundled aggregation of nanocellulose. The findings from the aforementioned study can be likened to the work by Bandera *et al.*, which showed a mechanochemistry approach (*i.e.*, sonication) to transform MCC into CNCs and nano-fibrillated cellulose (NFCs).[27] The SWE process has also been used to understand the effect of cellulose allomorph (cellulose I, II, II, and IV) on the hydrolysis of cellulose, where water at a subcritical state was used to cleave the 1,4-β-glycosidic bonds to convert the glucose intermediates.[28]

However, other studies have reported low rates of cellulose hydrolysis in non-catalyzed subcritical water since hydrolysis of ether bonds occurs at near-critical or supercritical conditions (T_C = 374.2 °C; P_C = 22.1 MPa),[29] where the cellulose decomposition rate is higher and more random.

Therefore, to exploit the SWE process for low-value woody biomass (*e.g.*, bleached pulp) to produce high-value CNCs, herein, we propose an SWE treatment of wood pulp in the presence of a Brønsted acid as a catalyst, to improve the extraction efficiency. In this work, we present the production of CNCs from bleached softwood pulps (as a model woody biomass) using acid-catalyzed SWE nanotechnology. Also, we have varied the temperature–time paradigm to understand the effect of process parameters on the morphology and degradation of the nanomaterials. To complement our engineered process, multi-modal characterization techniques, which are *inter alia*, electron microscopy, vibrational spectroscopy, and thermal analysis were performed to elucidate the morphology and physical properties of the CNCs. In most cases, SWE-derived CNCs were benchmarked against commercial nanocellulose (abbreviated as S-CNC, S corresponds to sulfuric acid). Hence, the manuscript is divided primarily into two parts – subcritical water hydrolysis of woody biomass (process), and physico-chemical analysis (characterization) of the isolated CNCs. We believe that the results from this method and the properties of the isolated nanoparticles offer promising and sustainable alternatives to the conventional production of cellulose nanocrystals. The suitability of this modified SWE nanotechnology can also extend to lignocellulosic biomass (that is, unbleached Kraft pulp and or plant fibers).

Experimental

Materials and methods

Northern Bleached Softwood Kraft pulp (NBSK) sheets were obtained from Canfor Corporation (Prince George Pulp Mill, BC, Canada) and used as the woody biomass in this experiment. Orthophosphoric acid (85 wt% v/v), Whatman glass microfiber filter membranes, Grade GF/B (1 μm), poly (allylamine hydrochloride) (PAH, MW 120 000–200 000 g mol^{-1}), and dialysis tubing cellulose membrane (molecular weight cut-off: 14 kDa) were purchased from Sigma Aldrich (Burlington, MA, USA).

Subcritical water hydrolysis of wood pulp. NBSK pulp sheets were milled (hereinafter labeled as Milled pulp) with a Wiley® mini mill from Thomas Scientific, USA (model: 1171H10) and sieved through a 40-mesh sieve before subcritical water treatment. Then, 2 g was employed as feedstock and later soaked in 200 mL reverse osmosis (RO) water containing 0.1 M orthophosphoric acid solution. After that, the pulp slurry was transferred into a batch reactor from Parr (4575 series, 500 mL capacity) as illustrated in Scheme 1.

The SWE process (acid-catalyzed) was carried at a constant inlet pressure of 14 MPa with varying temperatures from 120 °C, 150 °C and 170 °C (heating rate of approximately 4, 5, and 5.7 °C min^{-1} respectively), bringing the final reaction pressure to 18–19 MPa depending on the reaction temperature; reaction times of 60 and 120 min were used to investigate time effects on nanomaterial sizes bringing the total reaction times to 90 and 150 min respectively. Reaction conditions are shown in Table 1. In their earlier work, Novo *et al.*, reported the highest conversion of CNCs was achieved at a reaction pressure of 20.3 MPa.

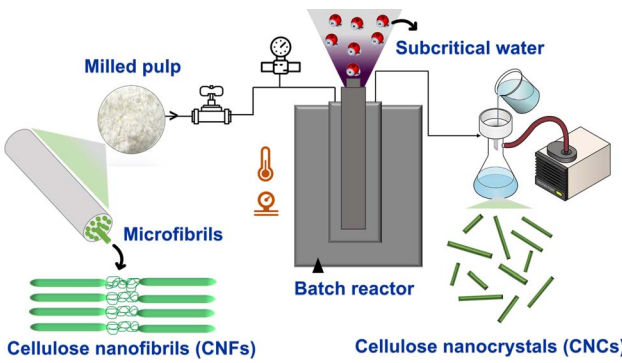

Scheme 1 Subcritical water extraction (SWE) process of NBSK bleached pulp (milled pulp) to cellulose nanocrystals.

Table 1 Reaction conditions for acid-catalyzed subcritical water digestion of bleached softwood pulp

Sample	Subcritical water temperature (°C)	Reaction time (min)	Reaction pressure (psi)	Acid concentration (wt% v/v)	Water : pulp ratio (ml g^{-1})
120 °C-60 min	120	60	2600	1	100 : 1
135 °C-60 min	135	60	2600	1	100 : 1
150 °C-60 min	150	60	2800	1	100 : 1
120 °C-120 min	120	120	2600	1	100 : 1
150 °C-120 min	150	120	2800	1	100 : 1

Considering this, a control experiment at 120 °C and 20.3 MPa for 30 min was performed to observe the effect of pressure on CNC conversion.

The hydrolyzed material was washed several times to achieve a neutral pH, sonicated using Branson Ultrasonics™ probe Sonifier™ SFX550, and stored at −31 °C for a minimum of 50 hours before lyophilization (Labconco FreeZone 4.5 L benchtop freeze system) for 72 hours. The freeze-dried sample was redispersed in water and cellulose nanocrystals were separated by filtering with a Buchner funnel fitted with a 1 μm glass microfiber ashless filter to obtain a CNC suspension. The suspensions were stored at 4 °C between analyses.

Multi-modal characterization of cellulose nanomaterials

Microscopic characterization: focus on morphology, aspect ratio, and size distribution

Scanning electron microscopy. To visualize the morphological and surface structure changes of subcritical water-treated microfibers, a scanning electron microscope with a secondary electron detector from FEI, USA (model: Helios NanoLab 650) was used. Freeze-dried hydrolyzed materials were screened using a sieve (100 μm mesh) and dispersed in DI water to make suspensions of 0.001 wt% before drop casting on double-sided carbon tapes (TED PELLA, Inc., ϕ 12.0 mm outside diameter (OD)) mounted onto aluminum studs (TED PELLA, Inc., ϕ 12.7 mm) with a 3.2 mm pin. The samples were air-dried before coating. All samples were iridium coated (thickness: ∼12 nm) using a sputter coater from Leica, Germany (model: DM200) before imaging.

Transmission electron microscopy. Transmission electron microscopy (model: Hitachi Tecnai Spirit) was used to further confirm the morphology and size of the nanomaterials. Before imaging, CNC suspension was probe sonicated to ensure dispersion. 50.0 μL of this suspension was deposited onto 200-mesh copper TEM grids and left to stand for about 1 min before wicking of excess solution with clean-cut paper wedges and staining with uranyl acetate (3% aqueous solution, Electron Microscopy Science).

Atomic force microscopy. Morphology of nanomaterials isolated and obtained after Büchner filtration was investigated by atomic force microscopy (AFM). Sample preparations were performed according to the protocol reported by Vanderfleet *et al.* 2017.[18] A diluted solution of 0.01 wt% CNC suspended in ultra-pure water was spin-coated onto the wafers. AFM images were taken with Jupiter XR Atomic Force Microscope from Asylum Research, Oxford Instruments Company, Santa Barbara, USA (model). Phase and height images were recorded with FS-1500 AUD cantilever tips with spring constant (6.00 N m^{-1}) and resonance frequency (1500.00 Hz) in tapping mode.

Light-scattering characterization: focus on colloidal properties

Dynamic light scattering. Dynamic light scattering technique was used to determine the apparent sizes of the isolated nanomaterials to support particle size measurements from AFM and TEM images. Measurements were taken on 0.01 wt% CNC suspensions with a particle size analyzer from Malvern, UK (model: ZetaSizer Nano) at 25 °C. Three particle size measurements were taken for each sample.

Zeta potential measurements. The colloidal stability of the CNC suspensions was investigated by measuring zeta potential using the same instrument used for particle size analysis (*vide supra*) with 0.01 wt% CNC suspension (without salt). Smoluchowski theory[30] was used to convert the electrophoretic mobility of the particles to zeta potential. A total of three measurements were performed for each sample. Suspensions, the values reported in Table 1 range from −17.8 mV to −8.3 mV for the various conditions investigated.

Vibrational spectroscopic characterization: emphasis on structure, functional groups, and crystallinity

Steady-state fluorometry. Fluorometry was performed using a modular fluorometer (FLS1000, Edinburgh Instruments, UK) by leveraging the autofluorescence feature of the subcritical water-extracted nanocelluloses. Since in solid-state, particle size could induce variability in the emission spectrum, hence, all the materials were first sieved with a mesh size of 100 and then packed into a U-shaped half-plate at a 45° angle configuration. Emission spectrums were collected in the range of 350–750 nm at a 2 nm step. Lamp intensity (55–75 a.u.) was adjusted according to the emissivity of cellulosic materials to mitigate saturation of the detector (photomultiplier tube, PMT-90) while excitation and emission bandwidth were set at 3.5 nm and 1 nm, respectively. To avoid scattering artifacts, a long pass (370 LP) was employed during the collection of the emission spectrums.

Raman spectroscopy. To gain molecular-level information on the SWE-enabled nanocelluloses, Raman spectroscopy was performed using two different Raman systems. One with a 532 nm laser excitation wavelength housed in a Raman microscope from Renishaw, UK (model: inVia™ Raman confocal microscope) and the second one with a 785 nm excitation wavelength housed in a dispersive Raman spectrometer from Wasatch Photonics, USA (model: WP 785). Note that owing to the autofluorescence of the nanocelluloses Raman spectrums

under 532 nm laser excitation resulted in a broad spectrum without any observable Raman peaks, which was mitigated under 785 nm laser excitation.

Fourier transform infrared spectroscopy. The chemical composition of subcritical hydrolyzed materials and milled pulp was investigated using a Fourier-transform infrared spectrometer from PerkinElmer, USA (model: Frontier™) with an attenuated total reflectance (ATR) probe. Freeze-dried samples were carefully placed on the surface of the diamond crystal and secured tightly with the attached anvil, ensuring maximum contact between the sample and probe. The spectra readings were taken between 4000–650 cm^{-1} at a resolution of 4 cm^{-1}. 16 scans were performed for each sample.

Powder X-ray diffractometry. The crystallinity of the isolated nanoparticles was analyzed using powder X-ray diffraction (XRD). The measurements were performed with an X-ray diffractometer from Bruker, USA (model: D8-advance) operating at 40 kV and 40 A[31] in a Bragg–Brentano configuration. Diffractograms were recorded with a step size of 0.03° within the range of 5°–90°. The crystallinities of the materials were calculated using the Segal method[32] where apparent crystallinity is expressed using ratios between maximum intensities at 002 lattice diffraction (I_{002}) and amorphous contribution (I_{am}) intensities at a diffraction angle (2θ) of 22.8° and 18° according to the equation below:

$$x\mathrm{CI}(\%) = \frac{I_{200} - I_{am}}{I_{am}} \times 100$$

Thermal characterization: focus on thermal stability

Thermal analysis. Thermal degradation kinetics of the cellulose nanocrystals were investigated with a thermogravimetric analyzer TGA 550 (TA Instruments). Approximately 10–20 mg of freeze-dried samples were oven-dried for at least 60 min at 60 °C before experiments. The analyses were conducted under nitrogen gas at a flow rate of 10 mL min^{-1} and heated at 20 °C per min from 25 °C to 800 °C. The experiment was repeated for milled pulp as a reference for any changes in the degradation kinetics and S-CNCs for benchmarking.

Results and discussions

Physical change in coloration

Visible changes in coloration were observed after subcritical water treatment of the pulp fibers with varying temperatures. As shown in Fig. 1, the color of the freeze-dried powders changed from desirable white/off-white to less desirable brown and black with increasing temperatures from 120, 135, 150, and 170 °C, respectively. Under subcritical conditions, as temperature increases but maintained <300 °C cellulose undergoes slow pyrolysis, characterized by dehydration and formation of char in the absence of oxygen.[33] This char formation could be responsible for the darkening of the hydrolyzed powders at 150 and 170 °C. SEM shows visible fibrillation of cellulose fibre surfaces at lower temperatures and at 150 °C seen as what appears to be an agglomeration of nanoparticles. However, at 170 °C SEM shows small globular and irregularly shaped particles indicative of fiber destruction resulting from over hydrolysis and complete degradation of the fibers.

Morphological characterization

The shape of nanoparticles after subcritical water treatment with increasing hydrolysis conditions was investigated using TEM. As expected, all particles hydrolyzed under 170 °C showed rod/needle-like structures typical of CNCs isolated *via* acid hydrolysis and other methods. The observation of these needle-like structures is indicative of the removal of amorphous regions in the cellulose fiber, influenced by the hydrolysis conditions. The TEM images shown in Fig. 2 reveal more rod-like particles are produced with increasing reaction temperature and time. At constant time (60 min), increasing the subcritical temperature is seen to produce more individualized and shorter particles. This is due to the increased hydrolysis rate at higher temperatures,[34] meaning higher efficiency in the dissolution of the amorphous regions. Also, it is interesting to note that fiber digestion may be more random rather than selective at higher temperatures, which may be the cause of the

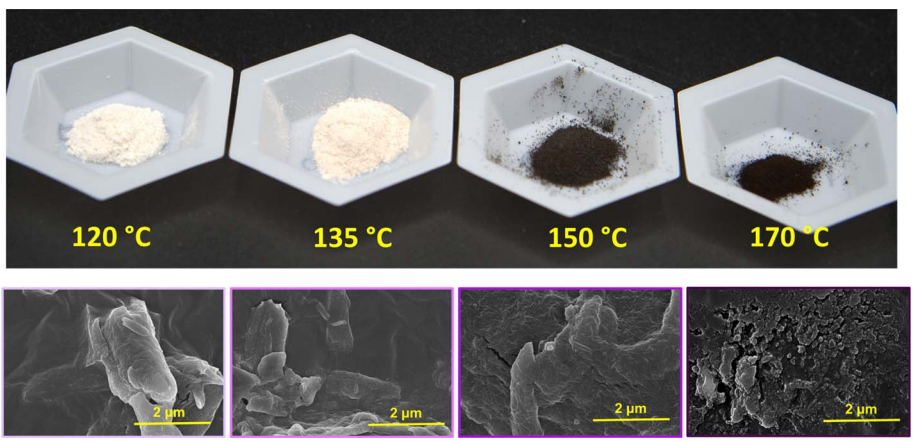

Fig. 1 Visible change in pulp whiteness after subcritical water treatment *via* various reaction temperatures (top image). Increasing reaction temperature resulted in increased fiber degradation observed in the severe darkening of hydrolyzed powders at higher temperatures. SEM images of hydrolyzed fibers (bottom image) corresponding to the investigated temperatures shown above. Fibrillation at fiber surfaces is increased with increasing temperatures up to 150 °C. Over hydrolysis and complete fiber degradation were observed at 170 °C.

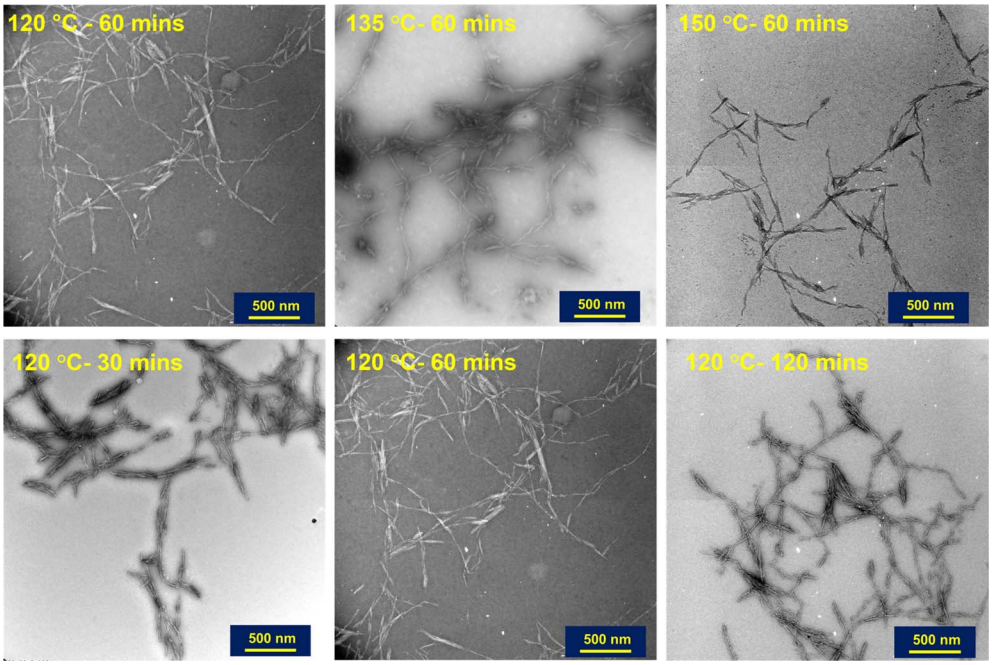

Fig. 2 TEM images of negatively stained cellulose nanocrystals showing the effects of increasing reaction temperature (top row) and time (bottom row) on nanoparticle morphology. Dispersed suspensions of nanoparticles in water were used for imaging.

reduction in the particle sizes observed at these temperatures. It is also important to note that the darkening of the hydrolyzed powders observed at 150 °C (Fig. 1) did not affect the overall morphology of the nanoparticles. At lower temperatures and pressures, increasing reaction time from 60–120 min produced more individualized rod-like particles. However, the same effect is seen at a reaction time of 30 minutes when the reaction pressure is slightly increased, possibly indicating pressure and prolonged reaction time might have similar effects in subcritical water hydrolysis of cellulose nanocrystals.

Particle size distribution

AFM was used to further confirm the morphology of nanocrystals and the size distribution of the particles (lengths) was analyzed using ImageJ software.[35] The particle size distributions were measured for each condition with three images showing different grid areas with a total of 90 particles. Fig. 3 shows the effect of reaction time on the particle lengths at 120 and 150 °C. From the distribution curves obtained, increasing the reaction time from 60 to 120 minutes shifts the bell curve from a zero skew (normal distribution) to a right skew (lognormal distribution) regardless of the temperature. Increasing reaction time produces more individualized particles with smaller sizes,[18] with reduced tendency of agglomeration. The median particle lengths for the various subcritical water reaction conditions investigated are presented in Table 2. The median lengths and aspect ratios reported in the table were also analyzed using SMART image analysis[36] to support manual measurements from ImageJ. We note here that given the aggregation of our nanoparticles; SMART was only used as a supporting analysis software.

Colloidal stability

Zeta potential measurements were used to assess the colloidal stability of the nanocrystals, calculated from the electrophoretic mobility of cellulose nanocrystals. The zeta potential values for the isolated CNCs are reported in Table 2. These values fall within a range that generally indicates the lack of colloidal stability for cellulose nanocrystals,[18] a property that is often influenced by the acid type and concentration. Given that only tiny amounts of phosphoric acid are used in the presence of excess water, the side esterification that often provides grafting of surface groups was greatly impeded, and as such little to no functional surface groups exist on the particles as seen from conductometric titration (ESI Fig. S8 and S9†).

Molecular level analysis: conversion of woody biomass into cellulose nanocrystals

Vibrational spectroscopic techniques, such as IR, Raman, and fluorescence can be utilized to understand the molecular-level structural information about the CNCs, which does not preclude other techniques, such as NMR.[37] With infra-red spectroscopy, it is challenging to discern between cellulosic nanomaterials (extracted materials) and milled pulps (woody biomass source) since they share similar functional groups, as shown in ESI Fig. S4.† On the other hand, Raman spectroscopy[38] inherently suffers from a fluorescence background. Thus, by leveraging the autofluorescence of CNCs, we investigated SWE-derived CNCs with fluorescence spectroscopy (Fig. 4), which has recently been shown to be sensitive to their physico-chemical properties.[39] In the case of CNCs (extracted materials), the solid-state emission spectrum was blue-shifted with temperature and pressure increase (Fig. 4a and b), which was confirmed

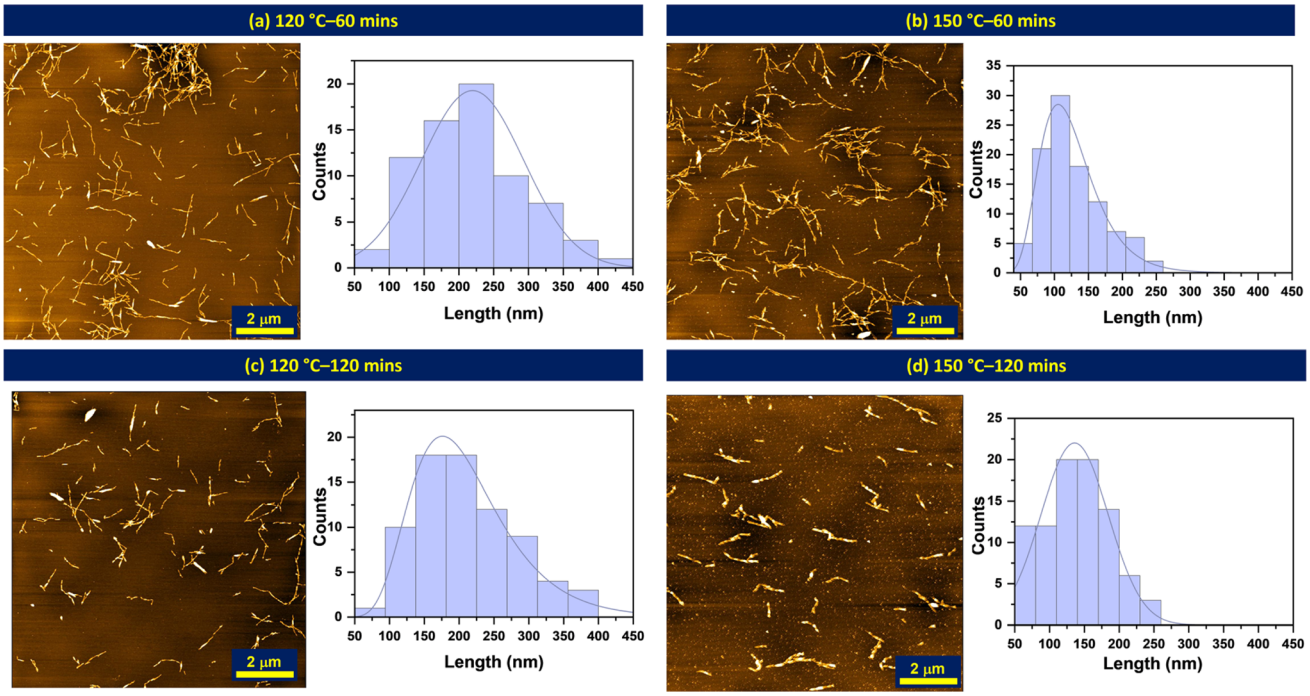

Fig. 3 AFM images of spin-coated subcritical water hydrolyzed CNCS showing the effect of reaction time (down the column) and subcritical temperature (across row) on particle size distribution. Histograms presented show the size distribution in particle lengths for each subcritical water condition. The size measurements were performed using ImageJ ($n = 90$).

Table 2 Physical properties of subcritical water hydrolyzed CNCs with varying reaction parameters (the conditions presented here are chosen to represent the effects of the average and harshest conditions used)

Reaction conditions	Median particle length (nm)	Width (nm)	Aspect ratio	Apparent DLS size (nm)	Zeta potential (mV)
120 °C-60 min	219 ± 73	12	18	337 ± 6	−8.01 ± 1
135 °C-60 min	132 ± 48	20	7	342 ± 36	−11.73 ± 0.7
150 °C-60 min	126 ± 44	15	9	311 ± 5	−10.6 ± 0.5
120 °C-120 min	210 ± 71	10	20	277 ± 8	−13.7 ± 0.7
150 °C-120 min	136 ± 48	18	7	297 ± 8	−17.8 ± 0.9

by employing reference cellulosic materials (Milled pulp, alpha-cellulose, and cellobiose in Fig. 4c) – time might not have a significant effect on nanomaterials yield or cellulose conversion, the temperature has a degree of influence, as seen for samples hydrolyzed at 120 and 135 °C. Interestingly, even at a relatively lower temperature (120 °C) and time (30 min), increasing the reaction pressure significantly affected the conversion, which further confirms the work by Novo *et al.*,[40] who confirmed that subcritical pressure mainly influenced the yield of cellulose nanocrystals. Finally, Raman spectroscopy (Fig. 4a and b) further confirmed cellulose I allomorph in the extracted CNCs irrespective of the process conditions.[38]

Crystalline phase analysis

The crystallinity of the nanoparticles produced from milled pulp *via* subcritical water treatment was investigated using powder X-ray diffraction (XRD) analysis. XRD provides useful information about the crystal size, structure, and orientation of a material. The diffractograms of untreated and subcritical water-treated materials are presented in Fig. 5.

Overall, the cellulose materials investigated showed peak intensities assigned to (002) crystal plane at $2q = 22.8°$, (101) at $2q = 14°–17°$ and some contributions at (040) only for subcritical water-treated fibers at $2q = 34.4°$. These represent characteristic peaks typical of cellulose I materials, the naturally existing allomorph of cellulose found in plants and other organisms. From the diffractograms shown above, the crystallinity of the untreated fibers increased significantly after subcritical water treatment. This increase in crystallinity can be attributed to the removal of amorphous contributions from the fiber chains, a consequence of hydrothermal hydrolysis, leaving more crystalline regions of the nanofibers. So far, the reaction conditions investigated are seen to have similar effects on the material's crystallinity with *ca.* 10% increase with increasing time. The highest crystallinity (73%) is observed at 135 °C which indicated maximum hydrolysis and removal of amorphous regions without significant damage to the nanocrystals.

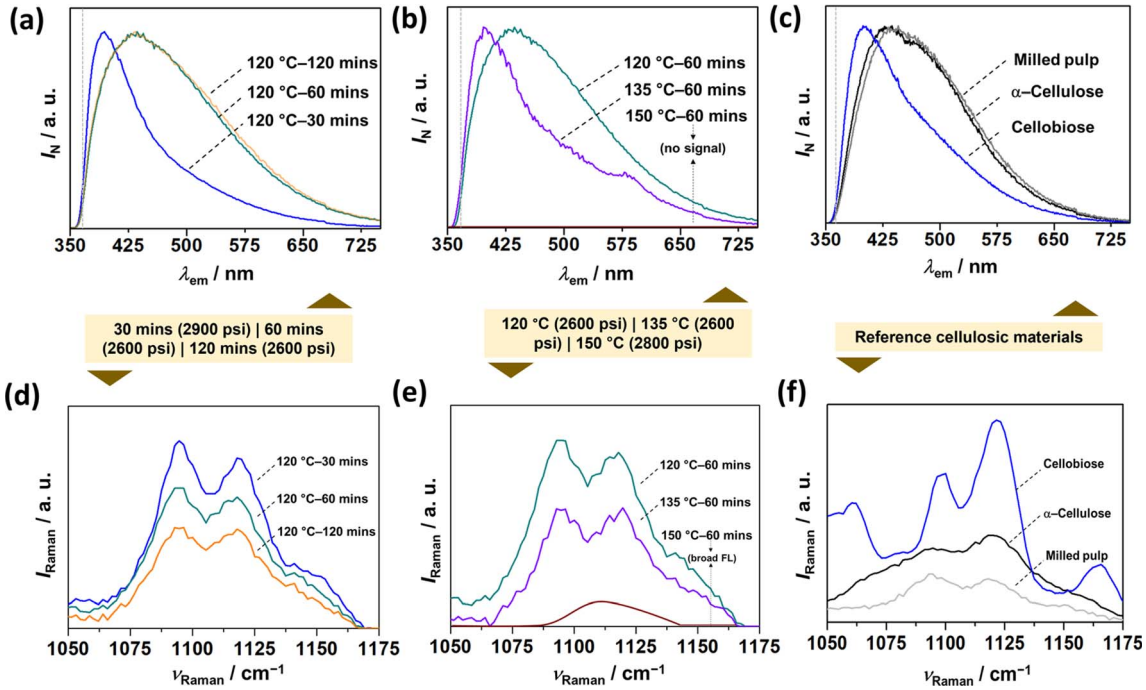

Fig. 4 Vibrational spectroscopic characterization of CNCs and reference materials. Steady-state emission (fluorescence) spectrums of (a and b) SWE CNCs as a function of (a) reaction time, (b) reaction temperature, and (c) reference cellulosic materials. Raman spectrums of (d and e) SWE CNCs as a function of (d) reaction time, (e) reaction temperature, and (f) reference materials. The colored box juxtaposition between the top and bottom figures indicates the operating pressure during each experiment. Reference materials include milled pulp, α-cellulose, and cellobiose. Note that α-cellulose and cellobiose serve as the reference for milled pulp, and CNCs respectively. The dotted grey-colored horizontal lines in (a)–(c) corresponds to the long-pass (LP) filter, *i.e.*, 370 LP. The Raman spectral region (1050–1175 cm^{-1}) covers the observable peaks corresponding to SCW-derived CNCs owing to large background fluorescence (see, ESI Fig. S3 and S4†).

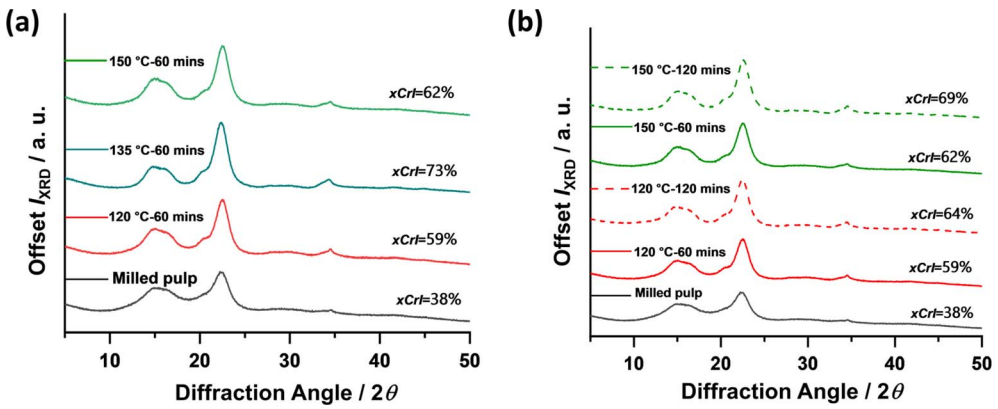

Fig. 5 XRD diffractograms showing the effect of temperature (a) and time (b) on the crystallinity of cellulose pulp before and after subcritical water treatment. Crystallinity values are calculated using intensity peaks according to Segal's equation.

However, further increase in temperature at 150 °C reduced the crystallinity, which may be a result of excessive hydrolysis, indicative that higher temperatures might have negative effects on nanoparticle crystallinity. Conditions investigated are seen to have similar effects on the material's crystallinity with *ca.* 10% increase with increasing time.

Thermal analysis

Thermogravimetric analysis (TGA) has been the standard method over the years to investigate the thermal behavior of cellulose and other natural and synthetic materials. TGA provides the thermal kinetics, decomposition temperature, and overall thermal stability of materials by measuring the change in weight of a material with increasing temperature and time. TGA of pure cellulose and its derivatives typically shows thermal degradation in the air within 300–500 °C, with maximum weight loss occurring around 400 °C or lower depending on the surface groups present, degree of crystallinity, and presence of impurities. The thermal stabilities of subcritical water CNCs hydrolyzed at 120, 135, and 150 °C for 60 min were investigated

relative to the starting milled pulp and compared to sulfuric acid hydrolyzed CNCs (S-CNCs). The thermal degradation curves and their first derivatives are shown in Fig. 6. All samples including untreated pulp showed one-step thermal degradation typical of pure cellulosic materials. As expected, S-CNCs showed the least thermal stability with T_{onset} occurring around 256 °C and maximum decomposition temperature T_{max} around 304 °C. Subcritical water hydrolysed CNCs showed relatively higher thermal stability with T_{onset} and T_{max} around 300 °C and 350 °C, respectively for samples hydrolysed at 120 °C. From the thermal degradation curves shown above, increasing subcritical water temperature did not significantly affect the T_{onset} for 135 °C and 150 °C at 280 and 270 °C, respectively. However, the effect of reaction temperature is seen in rate of weight loss during thermal degradation. At higher reaction temperatures (150 °C), weight loss/thermal decomposition is faster and the CNCs follow similar degradation as observed for S-CNCs. This can be attributed to the char formation at higher temperatures during subcritical treatment, responsible for the initial darkening of the powders. This phenomenon (char formation) is reported to be the cause of the low thermal stability of sulfuric acid hydrolyzed CNCs,[19] where the presence of char-forming sulfur groups on the CNCs impact their thermal stability.

Theoretical economic assessment of the proposed method

To assess the general economic feasibility of SWE to produce cellulose nanocrystals, Novo *et al.*,[21] reported a theoretical energy requirement of 424.8 MJ for the production of 30 kg of nanocellulose from 100 kg of material per hour. A comparison of their evaluation to conventional acid hydrolysis showed that energy requirements were significantly lower (43.2 MJ) for the same amount of material. However, regardless of the relatively higher energy requirements for SWE, the cost of nanocellulose produced from microcrystalline cellulose according to their cost analysis, considering all other necessary process conditions was significantly reduced (about 77-fold lower than sulfuric acid hydrolysed nanocellulose).

In this current work, we report equivalent energy requirements as process parameters were only adopted from this previous work. However, to account for the use of catalytic amounts of acid (1 wt%) used in this study and subsequent washing steps, the cost of CNC produced from this work could be about 26-fold lower costing about 0.06 \$ kg^{-1} of CNC compared to conventional industrial sulfuric acid isolated CNCs with 64 wt% acid produced for 1.54 \$ kg^{-1} CNC. The cost analysis is shown in ESI Table S1,† with all operational costs adapted from.[21] It is important to note that, this study not only provides an alternative approach to produce CNCs (with

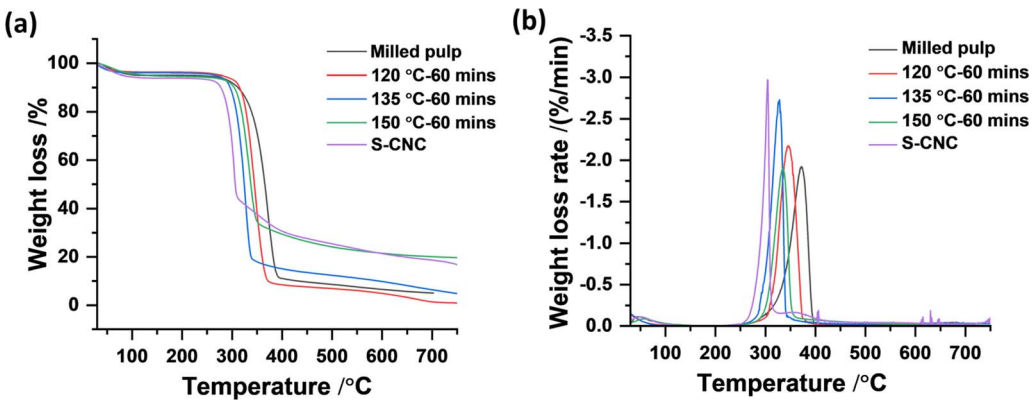

Fig. 6 Thermal degradation curves of CNCs and milled pulp (a) and rate of weight loss curves as a function of temperature showing maximum decomposition temperature for subcritical and acid hydrolyzed CNCs (b).

Table 3 Benchmarking acid-catalyzed subcritical water CNCs against conventional CNC extraction methods. The values shown are typical expected values reported in the literature for optimum conditions from the various methods and are dependent on experimental conditions

Methods of extraction	Maximum CNC yield	Aspect ratio	Onset of thermal degradation	Apparent crystallinity	Energy requirements (MJ)	Solvent requirement/g biomass
Acid-catalyzed SWE of wood pulp[a]	28–50	12 ± 18	300	68–73	~425 (ref. 21)	0.5 mL (85% v/v)
Sulfuric acid hydrolysis of wood pulp[41]	50–70	27 ± 9	270	75	~43 (ref. 21)	20 mL (95–98% w/w)
Phosphoric acid hydrolysis of cotton[19]	76–80	11 ± 15	290	81	~43 (ref. 21)	57.35 mL (85% v/v)
Enzymatic hydrolysis[42]	15.5	n/a	285	87.3–93.4	~30 (ref. 43)	0.2 wt% enzyme solution
Ionic solvent extraction[44]	~44	22–65	n/a	~73	—	5% w/w

[a] Property range is dependent on subcritical water reaction temperature. This current range represents the expected properties of CNCs hydrolyzed between subcritical water temperatures of 135 °C and 150 °C.

comparable properties with conventional methods as shown in Table 3) at a lower cost but also offers avenues for a sustainable conversion of other pure cellulosic biomasses like cotton and bleached plant fibres to cellulose nanocrystals.

Conclusions

In this work, we have shown that acid-catalysed subcritical water-based nanotechnology is an undoubtedly promising alternative to the sustainable production of cellulose nanomaterials from biomass residues. With about 98% solvent reduction from conventional CNC production methods, the current study successfully produces cellulose nanocrystals from bleached wood pulp, with physical and bulk properties of the nanomaterials are comparable to other conventional methods. In this work, we investigated the effects of subcritical water temperatures from 120 to 150 °C treatment durations of 60 and 120 min, and pressures between 2800–3000 psi on the physical and bulk properties of bleached wood pulp. The experimental findings show that generally, as observed in acid hydrolysis of biomass, increasing reaction conditions not only increases cellulose degradation but also significantly influences the properties of the isolated nanoparticles.

In this study, while the influence of reaction time was mostly observed through the dimensions of the nanoparticles isolated, the effect of temperature was rather significant in all other major properties, namely morphology, crystallinity, and thermal stability. Additionally, the nanoparticles produced in this work were shown to lack the needed colloidal stability typically expected of cellulose nanocrystals, which can be addressed by exploring the use of other weak acids or through post-modifications.

Moreover, we did not investigate the effect of pressure since all the experiments were performed with the same feed pressure. But the fluorometry studies performed for nanoparticles produced at slightly higher pressure (3000 psi) and shorter time (30 min) reveal higher conversion of the woody biomass (milled pulp) into smaller fragments which may be indicative of an increase in yield (of CNCs) at higher pressures. Further investigations are required to optimize process parameters and recipes to develop deeper insight into the conversion mechanism and to understand the role of non-cellulosic components (*e.g.*, hemicellulose, and lignin). Again, understanding the effects of biomass pretreatment to increase accessibility of cellulose chains to water molecules and role of organic catalysts like citric acid on the surface modification of isolated cellulose nanocrystals can advance this technology, improving its efficiency and economic viability for various applications.

Author contributions

Ruby Osei-Bonsu performed all experimental designs, sample preparation for characterization, AFM, TGA, FTIR, data analysis, writing, and editing. M. H. designed and performed SEM, fluorometry, and powder XRD experiments, data analysis, writing, and editing. Philip S. McMichael performed FTIR experiments and analysis, reviewing and editing. E. J. F. conceived the idea, contributed to editing, and acquired funding for this project. All authors have agreed to the final version of this manuscript.

Conflicts of interest

There are no conflicts of interest to declare.

Acknowledgements

The authors gratefully acknowledge the financial support provided by the NSERC Canfor Industrial Research Chair in Advanced Bioproducts, (# 553449-19), NSERC Discovery Grant (RGPIN-2021-03172), the Canada Foundation for Innovation (Project number 022176) and the Pacific Economic Development Canada (PacifiCan). Technical (and instrumental) support from Saeid Kamal (LASIR), Hooman TavakoliZadeh Noghabi (Ed Grant lab), Anita Lam (XRD laboratory), and Ben Herring (Shared Instrument Facility), Department of Chemistry, The University of British Columbia, Vancouver is gratefully appreciated. Dr Derrick Horne and Dr Naoji Yubuki from the UBC Bioimaging Facility are also acknowledged for TEM characterization.

References

1 T. Tabata, Environmental Impacts of Utilizing Woody Biomass for Energy: A Case Study in Japan, *Waste Biorefinery Potential and Perspectives*, 2018, pp. 751–778, DOI: 10.1016/B978-0-444-63992-9.00026-4.
2 A. Isogai, T. Saito and H. Fukuzumi, TEMPO-oxidized cellulose nanofibers, *Nanoscale*, 2011, **3**(1), 71–85, DOI: 10.1039/C0NR00583E.
3 T. Li, et al., Developing fibrillated cellulose as a sustainable technological material, *Nature*, 2021, **590**, 47–56, DOI: 10.1038/s41586-020-03167-7.
4 E. J. Foster, et al., Current characterization methods for cellulose nanomaterials, *Chem. Soc. Rev.*, 2018, **47**(8), 2609–2679, DOI: 10.1039/C6CS00895J.
5 L. Chen, Q. Wang, K. Hirth, C. Baez, U. P. Agarwal and J. Y. Zhu, Tailoring the yield and characteristics of wood cellulose nanocrystals (CNC) using concentrated acid hydrolysis, *Cellulose*, 2015, **22**(3), 1753–1762, DOI: 10.1007/S10570-015-0615-1.
6 A. Dufresne, Cellulose nanomaterial reinforced polymer nanocomposites, *Curr. Opin. Colloid Interface Sci.*, 2017, **29**, 1–8, DOI: 10.1016/J.COCIS.2017.01.004.
7 S. Das, B. Ghosh and K. Sarkar, Nanocellulose as sustainable biomaterials for drug delivery, *Sens. Int.*, 2022, **3**, 100135, DOI: 10.1016/J.SINTL.2021.100135.
8 M. C. Li, Q. Wu, K. Song, Y. Qing and Y. Wu, Cellulose nanoparticles as modifiers for rheology and fluid loss in bentonite water-based fluids, *ACS Appl. Mater. Interfaces*, 2015, **7**(8), 5009–5016, DOI: 10.1021/ACSAMI.5B00498.
9 D. Trache, M. H. Hussin, M. K. M. Haafiz and V. K. Thakur, Recent progress in cellulose nanocrystals: sources and production, *Nanoscale*, 2017, **9**(5), 1763–1786, DOI: 10.1039/C6NR09494E.

10 Y. Habibi, L. A. Lucia and O. J. Rojas, Cellulose Nanocrystals: Chemistry, Self-Assembly, and Applications, *Chem. Rev.*, 2010, **110**(6), 3479–3500, DOI: **10.1021/cr900339w**.

11 S. J. Eichhorn, Cellulose nanowhiskers: promising materials for advanced applications, *Soft Matter*, 2011, **7**(2), 303–315, DOI: **10.1039/C0SM00142B**.

12 D. Klemm, et al., Nanocelluloses: A new family of nature-based materials, *Angew. Chem., Int. Ed.*, 2011, **50**(24), 5438–5466, DOI: **10.1002/ANIE.201001273**.

13 S. Anderson, D. Esposito, W. Gillette, J. Zhu and U. Baxa, Enzymatic preparation of nanocrystalline and microcrystalline cellulose, *TAPPI J.*, 2014, DOI: **10.32964/TJ13.5.35**, **https://www.researchgate.net**.

14 I. A. Sacui, et al., Comparison of the properties of cellulose nanocrystals and cellulose nanofibrils isolated from bacteria, tunicate, and wood processed using acid, enzymatic, *ACS Publ.*, 2014, **6**(9), 6127–6138, DOI: **10.1021/am500359f**.

15 F. Beltramino, M. B. Roncero, A. L. Torres, T. Vidal and C. Valls, Optimization of sulfuric acid hydrolysis conditions for preparation of nanocrystalline cellulose from enzymatically pretreated fibers, *Cellulose*, 2016, **23**(3), 1777–1789, DOI: **10.1007/s10570-016-0897-y**.

16 J. Araki, M. Wada, S. Kuga and T. Okano, Flow properties of microcrystalline cellulose suspension prepared by acid treatment of native cellulose, *Colloids Surf., A*, 1998, **142**(1), 75–82, DOI: **10.1016/S0927-7757(98)00404-X**.

17 M. M. Mahmud, et al., Preparation of different polymorphs of cellulose from different acid hydrolysis medium, *Int. J. Biol. Macromol.*, 2019, **130**, 969–976, DOI: **10.1016/j.ijbiomac.2019.03.027**.

18 O. M. Vanderfleet, D. A. Osorio and E. D. Cranston, Optimization of cellulose nanocrystal length and surface charge density through phosphoric acid hydrolysis, *Philos. Trans. R. Soc., A*, 2018, **376**(2112), DOI: **10.1098/rsta.2017.0041**.

19 S. Camarero Espinosa, T. Kuhnt, E. J. Foster and C. Weder, Isolation of thermally stable cellulose nanocrystals by phosphoric acid hydrolysis, *Biomacromolecules*, 2013, **14**(4), 1223–1230, DOI: **10.1021/BM400219U**.

20 J. H. Jordan, M. W. Easson and B. D. Condon, Cellulose hydrolysis using ionic liquids and inorganic acids under dilute conditions: morphological comparison of nanocellulose, *RSC Adv.*, 2020, **10**(65), 39413, DOI: **10.1039/D0RA05976E**.

21 L. P. Novo, J. Bras, A. García, N. Belgacem and A. A. S. Curvelo, Subcritical Water: A Method for Green Production of Cellulose Nanocrystals, *ACS Sustain. Chem. Eng.*, 2015, **3**(11), 2839–2846, DOI: **10.1021/acssuschemeng.5b00762**.

22 A. V. Bandura and N. L. Serguei, *J. Phys. Chem.*, 2006, **35**, 15–30, DOI: **10.1063/1.1928231**.

23 S. B. Hawthorne, Y. Yang and D. J. Miller, Extraction of Organic Pollutants from Environmental Solids with Sub- and Supercritical Water, *Anal. Chem.*, 1994, **66**(18), 2912–2920, DOI: **10.1021/AC00090A019/ASSET/AC00090A019.FP.PNG_V03**.

24 Y. Pu, J. X. Wang, D. Wang, N. R. Foster and J. F. Chen, Subcritical water processing for nanopharmaceuticals, *Chem. Eng. Process.*, 2019, **140**, 36–42, DOI: **10.1016/j.cep.2019.04.013**.

25 O. Ahmadi and H. Jafarizadeh-Malmiri, Green approach in food nanotechnology based on subcritical water: effects of thyme oil and saponin on characteristics of the prepared oil in water nanoemulsions, *Food Sci. Biotechnol.*, 2020, **29**(6), 783–792, DOI: **10.1007/s10068-019-00727-0**.

26 S. Sohail Toor, L. Rosendahl and A. Rudolf, Hydrothermal liquefaction of biomass: A review of subcritical water technologies, *Energy*, 2011, **36**(5), 2328–2342, DOI: **10.1016/j.energy.2011.03.013**.

27 D. Bandera, et al., Influence of mechanical treatments on the properties of cellulose nanofibers isolated from microcrystalline cellulose, *React. Funct. Polym.*, 2014, **85**, 134–141, DOI: **10.1016/j.reactfunctpolym.2014.09.009**.

28 Y. Liu, H. Fu, W. Zhang and H. Liu, Effect of Crystalline Structure on the Catalytic Hydrolysis of Cellulose in Subcritical Water, *ACS Sustain. Chem. Eng.*, 2022, **10**(18), 5859–5866, DOI: **10.1021/acssuschemeng.1c08703**.

29 M. Sasaki, et al., Cellulose hydrolysis in subcritical and supercritical water, *J. Supercrit. Fluids*, 1998, **13**(1–3), 261–268, DOI: **10.1016/S0896-8446(98)00060-6**.

30 R. M. Mazo, Einstein–Smoluchowski Theory, *Brownian Motion*, 2008, pp. 46–61, DOI: **10.1093/ACPROF:OSO/9780199556441.003.0004**.

31 M. Deutsch, G. Hölzer, J. Härtwig, J. Wolf, M. Fritsch and E. Förster, *Kα* and *Kβ* x-ray emission spectra of copper, *Phys. Rev. A*, 1995, **51**(1), 283, DOI: **10.1103/PhysRevA.51.283**.

32 A. D. French and M. S. Cintrón, Cellulose polymorphy, crystallite size, and the Segal Crystallinity Index, *Cellulose*, 2013, **20**, 583–588, DOI: **10.1007/s10570-012-9833-y**.

33 L. K. Tolonen, Subcritical and Supercritical Water as a Cellulose Solvent, accessed: Mar. 24, 2023, **https://urn.fi/URN:ISBN:978-952-60-7025-4**.

34 T. Kobayashi, Y. Sakai and S. Asai, Hydrolysis rate of pentosan of hardwood in dilute sulfuric acid, *J. Agric. Chem. Soc. Jpn.*, 1956, **20**(1), 1–7, DOI: **10.1080/03758397.1956.10857296**.

35 Rasband, W.S. (1997-2015), ImageJ. National Institutes of Health, Bethesda, Maryland, USA, References - Scientific Research Publishing, **https://www.scirp.org/(S(czeh2tfqyw2orz553k1w0r45))/reference/ReferencesPapers.aspx?ReferenceID=1690059**, accessed Apr. 27, 2023.

36 S. Yucel, R. J. Moon, L. J. Johnston, B. Yucel and S. R. Kalidindi, Semi-automatic image analysis of particle morphology of cellulose nanocrystals, *Cellulose*, 2021, **28**, 2183–2201, DOI: **10.1007/s10570-020-03668-8**.

37 R. S. Dassanayake, Characterization of cellulose nanocrystals by current spectroscopic techniques, *Appl. Spectrosc. Rev.*, 2021, **58**(3), 180–205, DOI: **10.1080/05704928.2021.1951283**.

38 J. H. Wiley and R. H. Atalla, Band assignments in the Raman spectra of celluloses, *Carbohydr. Res.*, 1987, **160**(C), 113–129, DOI: **10.1016/0008-6215(87)80306-3**.

39 M. A. Johns, J. Abu-Namous, H. Zhao, M. Gattrell, J. Lockhart and E. D. Cranston, Autofluorescence spectroscopy for quantitative analysis of cellulose nanocrystals, *Nanoscale*, 2022, **14**(45), 16883–16892, DOI: **10.1039/D2NR04823J**.

40 L. P. Novo, J. Bras, A. García, N. Belgacem and A. A. da S. Curvelo, A study of the production of cellulose nanocrystals through subcritical water hydrolysis, *Ind. Crops Prod.*, 2016, **93**, 88–95, DOI: **10.1016/j.indcrop.2016.01.012**.

41 K.-H. Lin, T. Enomae and F.-C. Chang, Cellulose Nanocrystal Isolation from Hardwood Pulp using Various Hydrolysis Conditions, *Molecules*, 2019, **24**, 3724, DOI: **10.3390/molecules24203724**.

42 T. Yang, X. Li, N. Xu, Y. Guo, G. Liu and J. Zhao, Preparation of cellulose nanocrystals from commercial dissolving pulp using an engineered cellulase system, *Bioresour. Bioprocess.*, 2023, **10**, 42, DOI: **10.1186/s40643-023-00658-z**.

43 O. Rosales-Calderon, B. Pereira and V. Arantes, Economic assessment of the conversion of bleached eucalyptus Kraft pulp into cellulose nanocrystals in a stand-alone facility via acid and enzymatic hydrolysis, *Biofuels, Bioprod. Biorefin.*, 2021, **15**(6), 1775–1788, DOI: **10.1002/BBB.2277**.

44 H. Abushammala, I. Krossing and M.-P. Laborie, Ionic liquid-mediated technology to produce cellulose nanocrystals directly from wood, *Carbohydr. Polym.*, 2015, **134**, 609–616, DOI: **10.1016/j.carbpol.2015.07.079**.